Robotica (2011) volume 29, pp. 483–493. © Cambridge University Press 2010
doi:10.1017/S0263574710000330

The joint velocity, torque, and power capability evaluation of a redundant parallel manipulator

Yongjie Zhao†§* and Feng Gao‡

†Department of Mechatronics Engineering, Shantou University, Shantou City, Guangdong 515063, P. R. China
‡State Key Laboratory of Mechanical System and Vibration, Shanghai Jiao Tong University, Shanghai 200240, P. R. China
Email: fengg@sjtu.edu.cn
§Shantou Institute for Light Industrial Equipment Research, Shantou City, Guangdong 515021, P. R. China

(Received in Final Form: June 23, 2010. First published online: July 27, 2010)

SUMMARY

The evaluation of joint velocity, torque, and power capability of the 8-PSS redundant parallel manipulator is investigated in this paper. A series of new joint capability indices with obvious physical meanings are presented. The torque index used to evaluate the respective joint dynamic capability of the redundant parallel manipulator is decoupled into the acceleration, velocity, and gravity term. With these velocity, torque, and power indices, it is possible to control the respective joint capability of the redundant parallel manipulator in different directions. The indices have been applied to evaluate the joint capability of the redundant parallel manipulator by simulation. They are general and can be used for other types of parallel manipulators.

KEYWORDS: Rigid dynamics; Redundant parallel manipulator; Joint capability; Performance evaluation; Performance index.

1. Introduction

Performance is necessary to be considered when the parallel manipulator is developed. The performance index is fundamental to the performance evaluation. It is still an open problem.[1–3] For the fully parallel manipulator, there are two basic kinematic criteria: (i) the conditioning number, which is the ratio of the maximum singular value to the minimum singular value of the matrix. Gosselin and Angeles[4–5] adopted the condition number of the Jacobian matrix to evaluate the kinematic performance of the parallel manipulator and then defined the global conditioning index,[6] which can be implemented with a numerical technique. In order to avoid the unit inconsistency problem when using the condition number of the Jacobian matrix with nonhomogeneous physical units in the optimal design and control,[7–9] he derived a new Jacobian matrix and defined a new condition index[10] based on the principle that the plane is determined by three noncollinear points. The new conditioning index has been applied to the design of parallel manipulators.[11–13] (ii) The manipulability measures, the meanings of the manipulability can be interpreted as a measure of the manipulator capability for executing a specific task in a given configuration. Yoshikawa[14] defined the manipulability index as a generalized determinant of the Jacobian matrix and separated the total manipulability measure into translational and rotational manipulability.[15] Hong and Kim[16] defined a new manipulability measure, which included the total volume of a manipulability ellipsoid and the condition number of the Jacobian matrix, and optimized the Eclipse parallel manipulator by maximizing the manipulability measure. The definition of the above indices is that regarding all the input joints as one joint space in mathematics and investigating the mapping between the task space and the joint space.

The dynamic models are highly nonlinear, which make it difficult to predict the dynamic performance of the manipulator. However, the dynamic performance should be taken into account during the design to provide more advanced control and trajectory planning for the parallel manipulator. Borrowing ideas from the definition of the kinematic performance index, similar dynamic performance indices have been presented in the literatures.[17–27] Ma and Angeles[17–18] introduced the concept of a dynamic conditioning index, which was defined as the least square difference between the generalized inertia matrix and an isotropic matrix. Asada[19–20] introduced the generalized inertia ellipsoid as a tool to measure the capability of changing end-effector's velocity in different directions for a given kinetic energy. Yoshikawa[21] extended the concept of the kinematic manipulability ellipsoid to a dynamic manipulability ellipsoid for measuring the case of changing the end-effector's configuration by a set of joint torques with a fixed magnitude (2-norm). Huang and coworkers[22–23] adopted the maximum singular value of the generalized inertia matrix or its row vector matrix to evaluate the dynamic characteristic of the parallel manipulator. The key at the basis of the definition of the above performance measures is the generalized inertia matrix, which describes the mapping between the joint forces/torques and the end-effector accelerations. The velocity and gravity terms of the dynamic equations are not included in the rigid dynamic performance indices.

Redundancy can usually improve the ability and performance of a parallel manipulator.[28–37] It is believed that redundancy can bring some advantages for parallel manipulators such as avoiding kinematic singularities,

* Corresponding author. E-mail: meyjzhao@yahoo.com.cn

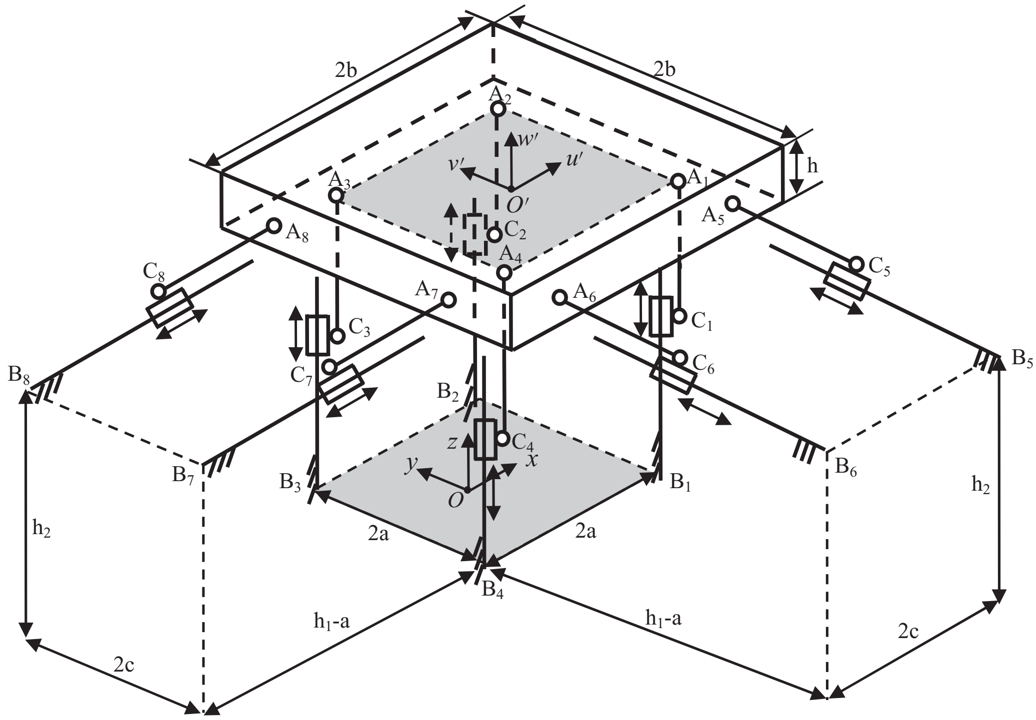

Figure 1. Schematic diagram of an 8-PSS redundant parallel manipulator.

increasing workspace, improving dexterity, enlarging load capability, and so on. Redundant parallel manipulators are usually overconstrained mechanisms, and the Jacobian matrix is not a square matrix. This will bring difficulties in the kinematics and dynamics analysis, especially for the dynamic performance evaluation. The above performance indices used for the fully parallel manipulator cannot be applied directly to the redundant parallel manipulator. In fact, there is little work on the performance evaluation of the redundant parallel manipulator.

This paper investigates the performance evaluation of the redundant parallel manipulator by computing the respective joint capability. The joint velocity, torque, and power capability of the 8-PSS redundant parallel manipulator are studied by means of a series of new indices with obvious physical meanings. The paper is organized as follows. Section 2 describes the 8-PSS redundant parallel manipulator. In Section 3, the kinematic model and rigid dynamic model are presented. Then the joint velocity, torque, and power capabilities are investigated in Section 3. Simulations and conclusions are given in Sections 4 and 5.

2. System Description

The 8-PSS redundant parallel manipulator is shown in Fig. 1. It consists of a moving platform and eight sliders. In each kinematic chain, the moving platform and the slider are connected via spherical ball bearing joints by a strut of fixed length. Each slider is driven by DC motor via linear ball screw. The lead screw of B_1, B_2, B_3, and B_4 are vertical to the ground. The lead screw of B_5, B_6 and the lead screw of B_7, B_8 are parallel with the ground. They are orthogonal to each other. The vector diagram of the PSS kinematic chain is shown in Fig. 2.

For the purpose of analysis, the following coordinate systems are defined: the coordinate system $O - xyz$ is attached

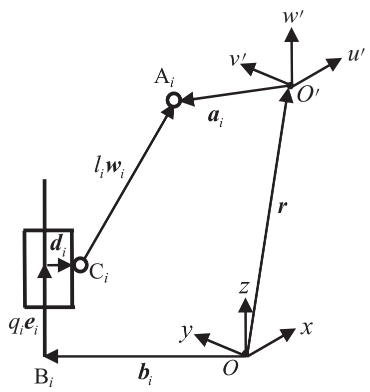

Figure 2. Vector diagram of a PSS kinematic chain.

to the fixed base, and another moving coordinate frame $O' - u'v'w'$ is located at the center of mass of the moving platform. The pose of the moving platform can be described by a position vector, $\boldsymbol{r}$, and a rotation matrix, ${}^{o}\boldsymbol{R}_{o'}$. Let the rotation matrix be defined by the roll, pitch, and yaw angles, namely, a rotation of ϕ_x about the fixed x axis, followed by a rotation of ϕ_y about the fixed y axis, and a rotation of ϕ_z about the fixed z axis. Thus, the rotation matrix is

$$
{}^{o}\boldsymbol{R}_{o'} = \mathrm{Rot}(z, \phi_z) \quad \mathrm{Rot}(y, \phi_y) \quad \mathrm{Rot}(x, \phi_x), \tag{1}
$$

where sϕ denotes the sine of angle ϕ, while cϕ denotes the cosine of angle ϕ. The angular velocity of the moving platform is given by[38]

$$
\boldsymbol{\omega} = [\dot{\phi}_x \quad \dot{\phi}_y \quad \dot{\phi}_z]^T. \tag{2}
$$

The orientation of each kinematic strut with respect to the fixed base can be described by two Euler angles. As shown

https://doi.org/10.1017/S0263574710000330 Published online by Cambridge University Press

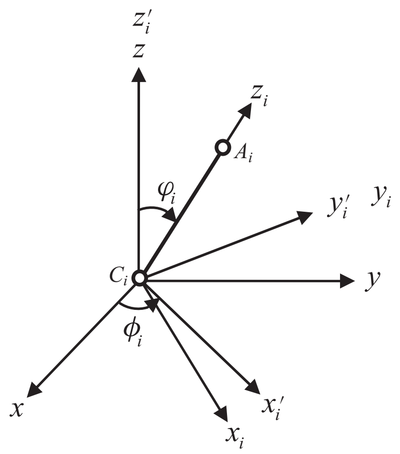

Figure 3. The local coordinate system of the ith strut.

in Fig. 3, the local coordinate systems of the ith strut can be thought of as a rotation of ϕ_i about the z-axis, resulting in a coordinate system $C_i - x_i'y_i'z_i'$ followed by another rotation of φ_i about the rotated y_i' axis. So the rotation matrix of the ith strut can be written as

$$^{o}\boldsymbol{R}_i = \mathrm{Rot}(z, \phi_i)\ \mathrm{Rot}(y_i', \varphi_i) = \begin{bmatrix} \mathrm{c}\phi_i \mathrm{c}\varphi_i & -\mathrm{s}\phi_i & \mathrm{c}\phi_i \mathrm{s}\varphi_i \\ \mathrm{s}\phi_i \mathrm{c}\varphi_i & \mathrm{c}\phi_i & \mathrm{s}\phi_i \mathrm{s}\varphi_i \\ -\mathrm{s}\varphi_i & 0 & \mathrm{c}\varphi_i \end{bmatrix}. \tag{3}$$

The unit vector along the strut in the coordinate system $O - xyz$ is

$$\boldsymbol{w}_i = {}^{o}\boldsymbol{R}_i {}^{i}\boldsymbol{w}_i = {}^{o}\boldsymbol{R}_i \begin{bmatrix} 0 \\ 0 \\ 1 \end{bmatrix} = \begin{bmatrix} \mathrm{c}\phi_i \mathrm{s}\varphi_i \\ \mathrm{s}\phi_i \mathrm{s}\varphi_i \\ \mathrm{c}\varphi_i \end{bmatrix}. \tag{4}$$

$$\boldsymbol{J}_x = \begin{bmatrix} \boldsymbol{w}_1 & \boldsymbol{w}_2 & \boldsymbol{w}_3 & \boldsymbol{w}_4 & \boldsymbol{w}_5 & \boldsymbol{w}_6 & \boldsymbol{w}_7 & \boldsymbol{w}_8 \\ \boldsymbol{a}_1 \times \boldsymbol{w}_1 & \boldsymbol{a}_2 \times \boldsymbol{w}_2 & \boldsymbol{a}_3 \times \boldsymbol{w}_3 & \boldsymbol{a}_4 \times \boldsymbol{w}_4 & \boldsymbol{a}_5 \times \boldsymbol{w}_5 & \boldsymbol{a}_6 \times \boldsymbol{w}_6 & \boldsymbol{a}_7 \times \boldsymbol{w}_7 & \boldsymbol{a}_8 \times \boldsymbol{w}_8 \end{bmatrix}^T, \tag{13}$$

So the Euler angles ϕ_i and φ_i can be computed as the following:

$$\begin{cases} \mathrm{c}\varphi_i = \boldsymbol{w}_{iz}, \\ \mathrm{s}\varphi_i = \sqrt{\boldsymbol{w}_{ix}^2 + \boldsymbol{w}_{iy}^2},\ (0 \le \varphi_i < \pi), \\ \mathrm{s}\phi_i = \boldsymbol{w}_{iy}/\mathrm{s}\varphi_i, \\ \mathrm{c}\phi_i = \boldsymbol{w}_{ix}/\mathrm{s}\varphi_i, \\ \text{if } \varphi_i = 0, \quad \text{then } \phi_i = 0. \end{cases} \tag{5}$$

3. Kinematic and Rigid Dynamic Model

3.1. Kinematics

3.1.1. Position analysis. As shown in Fig. 2, the closed-loop position equation associated with the ith kinematic chain can be written as follows:

$$\boldsymbol{r} + \boldsymbol{a}_i = l_i \boldsymbol{w}_i + \boldsymbol{b}_i + \boldsymbol{d}_i + q_i \boldsymbol{e}_i \quad i = 1, 2, \ldots, 8, \tag{6}$$

where $\boldsymbol{r}$, q_i, $\boldsymbol{e}_i$, $\boldsymbol{w}_i$, $\boldsymbol{a}_i$, $\boldsymbol{b}_i$, and $\boldsymbol{d}_i$ denote the vector $\boldsymbol{OO'}$, the joint variable, the unit vector along the lead screw, the unit vector along strut C_iA_i, the vector $\boldsymbol{O'A_i}$, the vector $\boldsymbol{OB_i}$, and the vector from the lead screw to the center point of the joint C_i, respectively.

3.1.2. Velocity analysis. Taking the derivative of Eq. (6) with respect to time yields

$$\dot{q}_i \boldsymbol{e}_i + \boldsymbol{\omega}_i \times l_i \boldsymbol{w}_i = \boldsymbol{v} + \boldsymbol{\omega} \times \boldsymbol{a}_i, \tag{7}$$

where $\boldsymbol{\omega}_i$ and $\boldsymbol{v}$ denote the angular velocity of the strut C_iA_i and the linear velocity of the moving platform, respectively.

Taking the dot product of both sides of Eq. (7) with $\boldsymbol{w}_i$ yields

$$\dot{q}_i = \begin{bmatrix} \dfrac{\boldsymbol{w}_i^T}{\boldsymbol{w}_i^T \boldsymbol{e}_i} & \dfrac{(\boldsymbol{a}_i \times \boldsymbol{w}_i)^T}{\boldsymbol{w}_i^T \boldsymbol{e}_i} \end{bmatrix} \begin{bmatrix} \boldsymbol{v} \\ \boldsymbol{\omega} \end{bmatrix}. \tag{8}$$

Rewriting Eq. (8) in the matrix form yields

$$\dot{\boldsymbol{q}} = \boldsymbol{J}_q^{-1} \boldsymbol{J}_x \dot{\boldsymbol{X}} = \boldsymbol{J} \dot{\boldsymbol{X}}, \tag{9}$$

where

$$\dot{\boldsymbol{q}} = [\dot{q}_1 \quad \dot{q}_2 \quad \dot{q}_3 \quad \dot{q}_4 \quad \dot{q}_5 \quad \dot{q}_6 \quad \dot{q}_7 \quad \dot{q}_8]^T, \tag{10}$$

$$\dot{\boldsymbol{X}} = \begin{bmatrix} \boldsymbol{v} \\ \boldsymbol{\omega} \end{bmatrix}, \tag{11}$$

$$\boldsymbol{J}_q = \mathrm{diag}\left(\boldsymbol{w}_1^T \boldsymbol{e}_1 \ \ \boldsymbol{w}_2^T \boldsymbol{e}_2 \ \ \boldsymbol{w}_3^T \boldsymbol{e}_3 \ \ \boldsymbol{w}_4^T \boldsymbol{e}_4 \ \ \boldsymbol{w}_5^T \boldsymbol{e}_5 \ \ \boldsymbol{w}_6^T \boldsymbol{e}_6 \ \ \boldsymbol{w}_7^T \boldsymbol{e}_7 \ \ \boldsymbol{w}_8^T \boldsymbol{e}_8\right), \tag{12}$$

$$\boldsymbol{J} = \boldsymbol{J}_q^{-1} \boldsymbol{J}_x = \begin{bmatrix} \boldsymbol{J}_1^T & \boldsymbol{J}_2^T & \boldsymbol{J}_3^T & \boldsymbol{J}_4^T & \boldsymbol{J}_5^T & \boldsymbol{J}_6^T & \boldsymbol{J}_7^T & \boldsymbol{J}_8^T \end{bmatrix}^T, \tag{14}$$

where $\boldsymbol{J}$ is the *Jacobian matrix*, which maps the velocity vector $\dot{\boldsymbol{X}}$ into the joint velocity vector $\dot{\boldsymbol{q}}$.

3.1.3. Link velocity analysis. The linear velocity of the point A_i in the coordinate system $C_i - x_iy_iz_i$ is

$${}^{i}\boldsymbol{v}_{Ai} = \dot{q}_i {}^{i}\boldsymbol{e}_i + {}^{i}\boldsymbol{\omega}_i \times l_i {}^{i}\boldsymbol{w}_i = {}^{i}\boldsymbol{v} + {}^{i}\boldsymbol{\omega} \times {}^{i}\boldsymbol{a}_i. \tag{15}$$

Since ${}^{i}\boldsymbol{\omega}_i^T {}^{i}\boldsymbol{w}_i = 0$, taking the cross product with ${}^{i}\boldsymbol{w}_i$ on both sides of Eq. (15), so the angular velocity of the link is obtained as

$$\begin{aligned} {}^{i}\boldsymbol{\omega}_i &= \frac{1}{l_i}\left({}^{i}\boldsymbol{w}_i \times {}^{i}\boldsymbol{v}_{Ai} - {}^{i}\boldsymbol{w}_i \times \dot{q}_i {}^{i}\boldsymbol{e}_i\right) \\ &= \frac{1}{l_i}\left(S\left({}^{i}\boldsymbol{w}_i\right){}^{i}\boldsymbol{v}_{Ai} - S\left({}^{i}\boldsymbol{w}_i\right)\dot{q}_i {}^{i}\boldsymbol{e}_i\right), \end{aligned} \tag{16}$$

where

$$S({}^i\boldsymbol{w}_i) = \begin{bmatrix} 0 & -{}^i w_{iz} & {}^i w_{iy} \\ {}^i w_{iz} & 0 & -{}^i w_{ix} \\ -{}^i w_{iy} & {}^i w_{ix} & 0 \end{bmatrix}. \tag{17}$$

Substituting Eqs. (8) and (15) into Eq. (16) yields

$$\begin{aligned} {}^i\boldsymbol{\omega}_i &= \frac{1}{l_i}\Big\{\left[S\left({}^i\boldsymbol{w}_i\right){}^i\boldsymbol{R}_o - S\left({}^i\boldsymbol{w}_i\right)S\left({}^i\boldsymbol{a}_i\right){}^i\boldsymbol{R}_o\right] \\ &\quad - \left({}^i\boldsymbol{w}_i \times {}^i\boldsymbol{e}_i\right)\left[\frac{\boldsymbol{w}_i^T}{\boldsymbol{w}_i^T\boldsymbol{e}_i} \;\; \frac{(\boldsymbol{a}_i \times \boldsymbol{w}_i)^T}{\boldsymbol{w}_i^T\boldsymbol{e}_i}\right]\Big\}\begin{bmatrix}\boldsymbol{v}\\ \boldsymbol{\omega}\end{bmatrix}, \\ &= \boldsymbol{J}_{i\omega}\begin{bmatrix}\boldsymbol{v}\\ \boldsymbol{\omega}\end{bmatrix} \end{aligned} \tag{18}$$

where

$$S({}^i\boldsymbol{a}_i) = \begin{bmatrix} 0 & -{}^i a_{iz} & {}^i a_{iy} \\ {}^i a_{iz} & 0 & -{}^i a_{ix} \\ -{}^i a_{iy} & {}^i a_{ix} & 0 \end{bmatrix}, \tag{19}$$

$${}^i\boldsymbol{R}_o = {}^o\boldsymbol{R}_i^{-1} = {}^o\boldsymbol{R}_i^T. \tag{20}$$

The velocity of the center of the ith strut in the coordinate system $C_i - x_i y_i z_i$ is

$${}^i\boldsymbol{v}_i = {}^i\boldsymbol{v}_{Ai} - {}^i\boldsymbol{\omega}_i \times \frac{l_i}{2}{}^i\boldsymbol{w}_i. \tag{21}$$

Substituting Eqs. (8), (15), and (18) into Eq. (21) yields

$$\begin{aligned} {}^i\boldsymbol{v}_i &= \left\{\left[{}^i\boldsymbol{R}_o - S\left({}^i\boldsymbol{a}_i\right){}^i\boldsymbol{R}_o\right] + \frac{l_i}{2}S\left({}^i\boldsymbol{w}_i\right)\boldsymbol{J}_{i\omega}\right\}\begin{bmatrix}\boldsymbol{v}\\ \boldsymbol{\omega}\end{bmatrix} \\ &= \boldsymbol{J}_{iv}\begin{bmatrix}\boldsymbol{v}\\ \boldsymbol{\omega}\end{bmatrix}. \end{aligned} \tag{22}$$

Rewriting the linear and angular velocity of the ith strut in the matrix form yields

$$\begin{bmatrix}{}^i\boldsymbol{v}_i\\ {}^i\boldsymbol{\omega}_i\end{bmatrix} = \begin{bmatrix}\boldsymbol{J}_{iv}\\ \boldsymbol{J}_{i\omega}\end{bmatrix}\begin{bmatrix}\boldsymbol{v}\\ \boldsymbol{\omega}\end{bmatrix} = \boldsymbol{J}_{iv\omega}\begin{bmatrix}\boldsymbol{v}\\ \boldsymbol{\omega}\end{bmatrix}, \tag{23}$$

where $\boldsymbol{J}_{iv\omega}$ is the *link Jacobian matrix*,[38] which maps the velocity of the moving platform in the task space into the velocity of the ith strut in the coordinate system $C_i - x_i y_i z_i$.

3.1.4. Acceleration analysis. Taking the derivative of Eq. (7) with respect to time gives

$$\begin{aligned} \dot{\boldsymbol{v}} &= \ddot{q}_i\boldsymbol{e}_i - \dot{\boldsymbol{\omega}} \times \boldsymbol{a}_i - \boldsymbol{\omega} \times (\boldsymbol{\omega} \times \boldsymbol{a}_i) + \dot{\boldsymbol{\omega}}_i \times l_i\boldsymbol{w}_i + \boldsymbol{\omega}_i \\ &\quad \times (\boldsymbol{\omega}_i \times l_i\boldsymbol{w}_i). \end{aligned} \tag{24}$$

Taking the dot product of both sides of Eq. (24) with $\boldsymbol{w}_i$ and simplifying yields

$$\begin{aligned} \ddot{q}_i &= \frac{1}{\boldsymbol{w}_i^T\boldsymbol{e}_i}\big(\boldsymbol{w}_i^T\dot{\boldsymbol{v}} + (\boldsymbol{a}_i \times \boldsymbol{w}_i)^T\dot{\boldsymbol{\omega}} + \boldsymbol{w}_i^T(\boldsymbol{\omega} \times (\boldsymbol{\omega} \times \boldsymbol{a}_i)) \\ &\quad - \boldsymbol{w}_i^T(\boldsymbol{\omega}_i \times (\boldsymbol{\omega}_i \times l_i\boldsymbol{w}_i))\big) \\ &= \boldsymbol{J}_i^T\begin{bmatrix}\dot{\boldsymbol{v}}\\ \dot{\boldsymbol{\omega}}\end{bmatrix} + \frac{1}{\boldsymbol{w}_i^T\boldsymbol{e}_i}\big((\boldsymbol{w}_i^T\boldsymbol{\omega})(\boldsymbol{a}_i^T\boldsymbol{\omega}) \\ &\quad - (\boldsymbol{w}_i^T\boldsymbol{a}_i)(\boldsymbol{\omega}^T\boldsymbol{\omega}) + l_i\,|\boldsymbol{\omega}_i \times \boldsymbol{w}_i|^2\big). \end{aligned} \tag{25}$$

Rewriting Eq. (25) in the matrix form yields

$$\ddot{\boldsymbol{q}} = \boldsymbol{J}\ddot{X} + \boldsymbol{V}, \tag{26}$$

where

$$\boldsymbol{V} = \begin{bmatrix}V_1 & V_2 & V_3 & V_4 & V_5 & V_6 & V_7 & V_8\end{bmatrix}^T, \tag{27}$$

$$V_i = \frac{1}{\boldsymbol{w}_i^T\boldsymbol{e}_i}\big((\boldsymbol{w}_i^T\boldsymbol{\omega})(\boldsymbol{a}_i^T\boldsymbol{\omega}) - (\boldsymbol{w}_i^T\boldsymbol{a}_i)(\boldsymbol{\omega}^T\boldsymbol{\omega}) + l_i\,|\boldsymbol{\omega}_i \times \boldsymbol{w}_i|^2\big). \tag{28}$$

3.1.5. Link acceleration analysis. Taking the derivative of Eq. (7) with respect to time in the coordinate system $C_i - x_i y_i z_i$ yields

$$\begin{aligned} {}^i\dot{\boldsymbol{v}} &= \ddot{q}_i{}^i\boldsymbol{e}_i - {}^i\dot{\boldsymbol{\omega}} \times {}^i\boldsymbol{a}_i - {}^i\boldsymbol{\omega} \times \left({}^i\boldsymbol{\omega} \times {}^i\boldsymbol{a}_i\right) + {}^i\dot{\boldsymbol{\omega}}_i \\ &\quad \times l_i{}^i\boldsymbol{w}_i + {}^i\boldsymbol{\omega}_i \times \left({}^i\boldsymbol{\omega}_i \times l_i{}^i\boldsymbol{w}_i\right). \end{aligned} \tag{29}$$

Taking the cross product with ${}^i\boldsymbol{w}_i$ on both sides of Eq. (29) yields

$$\begin{aligned} {}^i\dot{\boldsymbol{\omega}}_i &= \frac{1}{l_i}\big({}^i\boldsymbol{w}_i \times {}^i\dot{\boldsymbol{v}} - \left({}^i\boldsymbol{w}_i \times {}^i\boldsymbol{e}_i\right)\ddot{q}_i - {}^i\boldsymbol{w}_i \times \left({}^i\boldsymbol{a}_i \times {}^i\dot{\boldsymbol{\omega}}\right) \\ &\quad + {}^i\boldsymbol{w}_i\left({}^i\boldsymbol{\omega} \times \left({}^i\boldsymbol{\omega} \times {}^i\boldsymbol{a}_i\right)\right) - {}^i\boldsymbol{w}_i \times \left({}^i\boldsymbol{\omega}_i \times \left({}^i\boldsymbol{\omega}_i \times {}^i\boldsymbol{w}_i\right)\right)\big). \end{aligned} \tag{30}$$

Substituting Eq. (25) into Eq. (30) and simplifying yields

$${}^i\dot{\boldsymbol{\omega}}_i = \boldsymbol{J}_{i\omega}\begin{bmatrix}\dot{\boldsymbol{v}}\\ \dot{\boldsymbol{\omega}}\end{bmatrix} + \frac{1}{l_i}(\boldsymbol{\Delta}_1 + \boldsymbol{\Delta}_2), \tag{31}$$

where

$$\begin{aligned} \boldsymbol{\Delta}_1 &= -\frac{\left({}^i\boldsymbol{w}_i \times {}^i\boldsymbol{e}_i\right)}{\boldsymbol{w}_i^T\boldsymbol{e}_i}\big((\boldsymbol{w}_i^T\boldsymbol{\omega})(\boldsymbol{a}_i^T\boldsymbol{\omega}) - (\boldsymbol{w}_i^T\boldsymbol{a}_i)(\boldsymbol{\omega}^T\boldsymbol{\omega}) \\ &\quad + l_i\,|\boldsymbol{\omega}_i \times \boldsymbol{w}_i|^2\big), \end{aligned} \tag{32}$$

$$\boldsymbol{\Delta}_2 = \left({}^i\boldsymbol{\omega}_i^T{}^i\boldsymbol{a}_i\right)\left({}^i\boldsymbol{w}_i \times {}^i\boldsymbol{\omega}_i\right) - \left({}^i\boldsymbol{\omega}^T{}^i\boldsymbol{\omega}\right)\left({}^i\boldsymbol{w}_i \times {}^i\boldsymbol{a}_i\right). \tag{33}$$

Taking the derivative of Eq. (21) with respect to time yields

$$\begin{aligned} {}^i\dot{\boldsymbol{v}}_i &= {}^i\dot{\boldsymbol{v}}_{Ai} - \frac{l_i}{2}{}^i\dot{\boldsymbol{\omega}}_i \times {}^i\boldsymbol{w}_i - {}^i\boldsymbol{\omega}_i \times \left({}^i\boldsymbol{\omega}_i \times \frac{l_i}{2}{}^i\boldsymbol{w}_i\right) \\ &= {}^i\dot{\boldsymbol{v}} - S\left({}^i\boldsymbol{a}_i\right){}^i\dot{\boldsymbol{\omega}} + S({}^i\boldsymbol{\omega})S({}^i\boldsymbol{\omega}){}^i\boldsymbol{a}_i + \frac{l_i}{2}S\left({}^i\boldsymbol{w}_i\right){}^i\dot{\boldsymbol{\omega}}_i \\ &\quad - \frac{l_i}{2}S\left({}^i\boldsymbol{\omega}_i\right)S\left({}^i\boldsymbol{\omega}_i\right){}^i\boldsymbol{w}_i. \end{aligned} \tag{34}$$

Substituting Eq. (31) into Eq. (34) and simplifying yields

$$\begin{aligned} {}^i\dot{\boldsymbol{v}}_i &= \boldsymbol{J}_{iv}\begin{bmatrix}\dot{\boldsymbol{v}}\\ \dot{\boldsymbol{\omega}}\end{bmatrix} + S\left({}^i\boldsymbol{\omega}_i\right)S\left({}^i\boldsymbol{\omega}_i\right){}^i\boldsymbol{a}_i + \frac{1}{2}S\left({}^i\boldsymbol{w}_i\right)(\boldsymbol{\Delta}_1 + \boldsymbol{\Delta}_2) \\ &\quad - \frac{l_i}{2}S\left({}^i\boldsymbol{\omega}_i\right)S\left({}^i\boldsymbol{\omega}_i\right){}^i\boldsymbol{w}_i. \end{aligned} \tag{35}$$

3.2. Rigid dynamics

3.2.1. Applied and inertia wrenches. The resultant of applied and inertia forces exerted at the center of mass of the moving platform is

$$\boldsymbol{Q}_P = \begin{bmatrix} \boldsymbol{f}_P \\ \boldsymbol{n}_P \end{bmatrix} = \begin{bmatrix} \boldsymbol{f}_e + m_p \boldsymbol{g} - m_p \dot{\boldsymbol{v}} \\ \boldsymbol{n}_e - {}^o\boldsymbol{I}_p \dot{\boldsymbol{\omega}} - \boldsymbol{\omega} \times ({}^o\boldsymbol{I}_p \boldsymbol{\omega}) \end{bmatrix}, \quad (36)$$

where $\boldsymbol{f}_e$ and $\boldsymbol{n}_e$ are the external force and moment exerted at the center of mass of the moving platform, ${}^o\boldsymbol{I}_p = {}^o\boldsymbol{R}_{o'}{}^{o'}\boldsymbol{I}_p{}^{o'}\boldsymbol{R}_o$ is the inertia matrix of the moving platform taken about the center of mass expressed in the coordinate system $O - xyz$ and m_p is its mass.

The resultant of applied and inertia forces exerted at the center of mass of the ith strut can be expressed in the coordinate system $C_i - x_i y_i z_i$ as

$${}^i\boldsymbol{Q}_i = \begin{bmatrix} {}^i\boldsymbol{f}_i \\ {}^i\boldsymbol{n}_i \end{bmatrix} = \begin{bmatrix} m_i {}^i\boldsymbol{R}_o \boldsymbol{g} - m_i {}^i\dot{\boldsymbol{v}}_i \\ -{}^i\boldsymbol{I}_i {}^i\dot{\boldsymbol{\omega}}_i - {}^i\boldsymbol{\omega}_i \times ({}^i\boldsymbol{I}_i {}^i\boldsymbol{\omega}_i) \end{bmatrix}, \quad (37)$$

where ${}^i\boldsymbol{I}_i$ is the inertia matrix of the ith cylindrical strut about its respective center of mass expressed in the coordinate system $C_i - x_i y_i z_i$ and m_i is its mass.

There is pure translational motion for the slider, so the resultant of applied and inertia forces exerted at the center of mass of the slider can be expressed in the coordinate system $O - xyz$ as

$$f_{qi} = (m_{qi}\boldsymbol{g} - m_{qi}\ddot{\boldsymbol{q}}_i)^T \boldsymbol{e}_i, \quad (38)$$

where m_{qi} and $\ddot{\boldsymbol{q}}_i$ are the mass and the acceleration of the slider.

There is pure rotation motion for the lead screw, coupler, and motor rotor, so the resultant of applied and inertia forces exerted at the screw-coupler-rotor is

$$N_i = \tau_i - (I_{Li} + I_{Ci} + I_{Mi})\ddot{\theta}_i, \quad (39)$$

where I_{Li}, I_{Ci}, and I_{Mi} are the rotary inertia of the lead screw, coupler, and motor rotor, respectively, τ_i is the input torque actuated by the motor, $\ddot{\theta}_i$ is the angular acceleration of the screw-coupler-rotor. The relationship between the lead screw motion and the slider motion is $\ddot{\theta}_i = \left(2\pi / p_i\right) \ddot{q}_i$. Where $p_i = 0.05\ \text{m}^{-1}$ is the lead of the linear ball screw.

3.2.2. Equations of motion. According to D'Alembert's principle, the principle of virtual work can be extended from the static to the dynamic case. It can be stated as: The virtual work of the external forces applied to the system must be zero. For this redundant parallel manipulator, it can be expressed in the formula:

$$\delta\boldsymbol{x}_p^T \boldsymbol{Q}_p + \sum_{i=1}^{8} \delta^i \boldsymbol{x}_i^{T\,i} \boldsymbol{Q}_i + \delta\boldsymbol{Q}^T \boldsymbol{f}_q + \delta\boldsymbol{\theta}^T \boldsymbol{N} = 0, \quad (40)$$

where

$$\delta\boldsymbol{q} = \begin{bmatrix} \delta q_1 & \delta q_2 & \delta q_3 & \delta q_4 & \delta q_5 & \delta q_6 & \delta q_7 & \delta q_8 \end{bmatrix}^T, \quad (41)$$

$$\begin{aligned} \delta\boldsymbol{\theta} &= \begin{bmatrix} \delta\theta_1 & \delta\theta_2 & \delta\theta_3 & \delta\theta_4 & \delta\theta_5 & \delta\theta_6 & \delta\theta_7 & \delta\theta_8 \end{bmatrix}^T \\ &= \operatorname{diag}\left(\frac{2\pi}{p_1} \quad \frac{2\pi}{p_2} \quad \frac{2\pi}{p_3} \quad \frac{2\pi}{p_4} \quad \frac{2\pi}{p_5} \quad \frac{2\pi}{p_6} \quad \frac{2\pi}{p_7} \quad \frac{2\pi}{p_8} \right) \\ &= \boldsymbol{A}\delta\boldsymbol{q}, \end{aligned} \quad (42)$$

$$\boldsymbol{f}_q = \begin{bmatrix} f_{q1} & f_{q2} & f_{q3} & f_{q4} & f_{q5} & f_{q6} & f_{q7} & f_{q8} \end{bmatrix}^T, \quad (43)$$

$$\boldsymbol{N} = \begin{bmatrix} N_1 & N_2 & N_3 & N_4 & N_5 & N_6 & N_7 & N_8 \end{bmatrix}^T. \quad (44)$$

In Eq. (40), the resultant of the applied and inertia forces ${}^i\boldsymbol{Q}_i$ and its corresponding virtual displacement $\delta^i\boldsymbol{x}_i$ are expressed in the coordinate system $C_i - x_i y_i z_i$. From Eq. (23), the relationship between the above virtual displacement $\delta^i\boldsymbol{x}_i$ and the virtual displacement $\delta\boldsymbol{x}_p$ is determined by

$$\delta^i\boldsymbol{x}_i^T = \delta\boldsymbol{x}_p^T \boldsymbol{J}_{iv\omega}^T. \quad (45)$$

The relationship between the virtual displacement $\delta\boldsymbol{Q}$ and $\delta\boldsymbol{x}_p$ is

$$\delta\boldsymbol{Q}^T = \delta\boldsymbol{x}_p^T \boldsymbol{J}^T. \quad (46)$$

Substituting Eqs. (42), (45), and (46) into Eq. (40) yields

$$\delta\boldsymbol{x}_p^T \boldsymbol{Q}_p + \sum_{i=1}^{8} \delta\boldsymbol{x}_p^T \boldsymbol{J}_{iv\omega}^T {}^i\boldsymbol{Q}_i + \delta\boldsymbol{x}_p^T \boldsymbol{J}^T \boldsymbol{f}_q + \delta\boldsymbol{x}_p^T \boldsymbol{J}^T \boldsymbol{A}^T \boldsymbol{N} = 0. \quad (47)$$

Since Eq. (47) is always valid for any $\delta\boldsymbol{x}_p$, it must follow that

$$\boldsymbol{Q}_p + \sum_{i=1}^{8} \boldsymbol{J}_{iv\omega}^T {}^i\boldsymbol{Q}_i + \boldsymbol{J}^T \boldsymbol{f}_q + \boldsymbol{J}^T \boldsymbol{A}^T \boldsymbol{N} = 0. \quad (48)$$

Eq. (48) can be written as

$$\boldsymbol{J}^T \boldsymbol{A}^T \boldsymbol{\tau} = \boldsymbol{J}^T \boldsymbol{A}^T \boldsymbol{I}_{LCM} \ddot{\boldsymbol{\theta}} - \boldsymbol{Q}_p - \sum_{i=1}^{8} \boldsymbol{J}_{iv\omega}^T {}^i\boldsymbol{Q}_i - \boldsymbol{J}^T \boldsymbol{f}, \quad (49)$$

where

$$\boldsymbol{I}_{LCM} = \operatorname{diag}(I_{LCM1} \quad I_{LCM2} \quad I_{LCM3} \quad I_{LCM4} \quad I_{LCM5} \quad I_{LCM6} \quad I_{LCM7} \quad I_{LCM8}), \quad (50)$$

$$I_{LCMi} = I_{Li} + I_{Ci} + I_{Mi}. \quad (51)$$

There are eight unknown quantities in the six linear consistent equations. So the solution is infinite. The most common strategy to solve this kind of problem is by minimizing the

https://doi.org/10.1017/S0263574710000330 Published online by Cambridge University Press

Euclidian norm of the actuating torque vector:

$$\boldsymbol{\tau} = -\boldsymbol{A}^{-T}(\boldsymbol{J}^T)^{+}\left(\boldsymbol{Q}_p + \sum_{i=1}^{8} \boldsymbol{J}_{iv\omega}^{T}\, {}^{i}\boldsymbol{Q}_i + \boldsymbol{J}^T \boldsymbol{f}_q\right) + \boldsymbol{I}_{LCM}\ddot{\boldsymbol{\theta}}$$
$$= -\boldsymbol{A}^{-T}(\boldsymbol{J}^T)^{+}\left(\boldsymbol{Q}_p + \sum_{i=1}^{8} \boldsymbol{J}_{iv\omega}^{T}\, {}^{i}\boldsymbol{Q}_i + \boldsymbol{J}^T \boldsymbol{f}_q\right) + \boldsymbol{I}_{LCM}\boldsymbol{A}\ddot{q}. \quad (52)$$

The physical significance of the above equation is that among the possible actuating torque vectors, the optimum solution is that with minimum norm and least quadratic sum. The $\boldsymbol{J}^{+}$ is the Moore–Penrose inverse of the Jacobian matrix. Substituting Eqs. (36)–(39) into Eq. (52) yields

$$\begin{aligned}\boldsymbol{\tau} = {} & -\boldsymbol{A}^{-T}(\boldsymbol{J}^T)^{+}\begin{bmatrix}\boldsymbol{f}_e\\ \boldsymbol{n}_e\end{bmatrix} - \boldsymbol{A}^{-T}(\boldsymbol{J}^T)^{+}\left\{\begin{bmatrix} m_p\boldsymbol{g}\\ \boldsymbol{0}\end{bmatrix} + \sum_{i=1}^{8}\boldsymbol{J}_{iv\omega}^{T}\begin{bmatrix} m_i\,{}^{i}\boldsymbol{R}_o\boldsymbol{g}\\ \boldsymbol{0}\end{bmatrix}\right.\\ & \left. + \boldsymbol{J}^T[(m_{q1}\boldsymbol{g})^T\boldsymbol{e}_1 \quad (m_{q2}\boldsymbol{g})^T\boldsymbol{e}_2 \quad (m_{q3}\boldsymbol{g})^T\boldsymbol{e}_3 \quad (m_{q4}\boldsymbol{g})^T\boldsymbol{e}_4 \quad (m_{q5}\boldsymbol{g})^T\boldsymbol{e}_5 \quad (m_{q6}\boldsymbol{g})^T\boldsymbol{e}_6 \quad (m_{q7}\boldsymbol{g})^T\boldsymbol{e}_7 \quad (m_{q8}\boldsymbol{g})^T\boldsymbol{e}_8]^T\right\}\\ & + \boldsymbol{A}^{-T}(\boldsymbol{J}^T)^{+}\left\{\begin{bmatrix} m_p\dot{\boldsymbol{v}}\\ {}^{o}\boldsymbol{I}_p\dot{\boldsymbol{\omega}}\end{bmatrix} + \sum_{i=1}^{8}\boldsymbol{J}_{iv\omega}^{T}\begin{bmatrix} m_i\,{}^{i}\dot{\boldsymbol{v}}_i\\ {}^{i}\boldsymbol{I}_i\,{}^{i}\dot{\boldsymbol{\omega}}_i\end{bmatrix}\right.\\ & \left. + \boldsymbol{J}^T[m_{q1}\ddot{q}_1 \quad m_{q2}\ddot{q}_2 \quad m_{q3}\ddot{q}_3 \quad m_{q4}\ddot{q}_4 \quad m_{q5}\ddot{q}_5 \quad m_{q6}\ddot{q}_6 \quad m_{q7}\ddot{q}_7 \quad m_{q8}\ddot{q}_8] + \boldsymbol{I}_{LCM}\boldsymbol{A}\ddot{q}\right\}\\ & + \boldsymbol{A}^{-T}(\boldsymbol{J}^T)^{+}\left\{\begin{bmatrix}\boldsymbol{0}\\ \boldsymbol{\omega}\times({}^{o}\boldsymbol{I}_p\boldsymbol{\omega})\end{bmatrix} + \sum_{i=1}^{8}\boldsymbol{J}_{iv\omega}^{T}\begin{bmatrix}\boldsymbol{0}\\ {}^{i}\boldsymbol{\omega}_i\times({}^{i}\boldsymbol{I}_i\,{}^{i}\boldsymbol{\omega}_i)\end{bmatrix}\right\},\end{aligned} \quad (53)$$

where $\boldsymbol{0} = [0 \quad 0 \quad 0]^T$.

4. Joint Capability Evaluation

4.1. Joint velocity capability

The relationship between the input angular velocity of the motor rotor and the velocity of the moving platform is

$$\dot{\boldsymbol{\theta}} = \boldsymbol{A}\dot{q} = \boldsymbol{A}\boldsymbol{J}\dot{X} = \boldsymbol{J}_\theta\dot{\boldsymbol{X}}$$
$$= [\boldsymbol{J}_{\theta1} \quad \boldsymbol{J}_{\theta2} \quad \boldsymbol{J}_{\theta3} \quad \boldsymbol{J}_{\theta4} \quad \boldsymbol{J}_{\theta5} \quad \boldsymbol{J}_{\theta6}]\begin{bmatrix}\boldsymbol{v}\\ \boldsymbol{\omega}\end{bmatrix}, \quad (54)$$

where $\dot{\boldsymbol{\theta}}$ is the angular velocity of the motor rotor, $\boldsymbol{J}_\theta$ is the matrix, which maps the velocity of the moving platform into the angular velocity of the motor rotor, $\boldsymbol{J}_{\theta j}$ is the column vector component of the matrix $\boldsymbol{J}_\theta$.

When the moving platform translates along or rotates about the x, y, and z axes in the unit velocity, the input angular velocity of the motor rotor is

$$\dot{\boldsymbol{\theta}}_j = \boldsymbol{J}_\theta\boldsymbol{\chi}_j = \boldsymbol{J}_{\theta j}, \quad (j = 1, 2, \ldots, 6), \quad (55)$$

where

$$\chi_1 = [1 \quad 0 \quad 0 \quad 0 \quad 0 \quad 0]^T, \quad (56a)$$

$$\chi_2 = [0 \quad 1 \quad 0 \quad 0 \quad 0 \quad 0]^T, \quad (56b)$$

$$\chi_3 = [0 \quad 0 \quad 1 \quad 0 \quad 0 \quad 0]^T, \quad (56c)$$

$$\chi_4 = [0 \quad 0 \quad 0 \quad 1 \quad 0 \quad 0]^T, \quad (56d)$$

$$\chi_5 = [0 \quad 0 \quad 0 \quad 0 \quad 1 \quad 0]^T, \quad (56e)$$

$$\chi_6 = [0 \quad 0 \quad 0 \quad 0 \quad 0 \quad 1]^T \quad (56f)$$

are used to represent the unit linear and angular velocity of the moving platform when it translates along or rotates about the x, y, and z axes. They will also later be used to represent the unit linear and angular acceleration of the moving platform when it translates along or rotates about the x, y and z axes.

For the ith input joint ($i = 1, 2, \ldots, 8$)

$$\dot{\theta}_{i\chi_j} = \Big[\underbrace{0\cdots0}_{i-1} \quad 1 \quad \underbrace{0\cdots0}_{8-i}\Big]\boldsymbol{J}_{\theta j} = \boldsymbol{J}_{\theta ij} \quad (57)$$

is the input angular velocity of the ith joint when the unit velocity of the moving platform is $\boldsymbol{\chi}_j$.

So,

$$\dot{\theta}_{i\max} = \max\left(\left[\left|\boldsymbol{J}_{\theta_{i1}}\right|, \quad \left|\boldsymbol{J}_{\theta_{i2}}\right|, \quad \cdots \quad \left|\boldsymbol{J}_{\theta_{i6}}\right|\right]\right)$$
$$= \max\left(\left[\left|\dot{\theta}_{i\chi_1}\right|, \quad \left|\dot{\theta}_{i\chi_2}\right|, \quad \cdots \quad \left|\dot{\theta}_{i\chi_6}\right|\right]\right) \quad (58)$$

is the maximum input angular velocity of the ith joint when the velocity of the moving platform is unit. It is taken as the performance index to evaluate the ith joint velocity capability of the redundant parallel manipulator.

4.2. Joint rigid dynamic capability

4.2.1. Joint torque capability. Substituting Eqs. (23), (31), and (35) into Eq. (53) and simplifying, the inverse dynamic model of the redundant parallel manipulator is achieved

$$\boldsymbol{\tau} = \boldsymbol{M}(\boldsymbol{X})\ddot{\boldsymbol{X}} + \boldsymbol{V}(\boldsymbol{X}, \dot{\boldsymbol{X}}) + \boldsymbol{g}(\boldsymbol{X}) - \boldsymbol{A}^{-T}\boldsymbol{J}^{-T}\begin{bmatrix}\boldsymbol{f}_e\\ \boldsymbol{n}_e\end{bmatrix}$$
$$= \boldsymbol{\tau}_a + \boldsymbol{\tau}_v + \boldsymbol{\tau}_g + \boldsymbol{\tau}_e, \quad (59)$$

where

$$\boldsymbol{M}(\boldsymbol{X}) = \boldsymbol{A}^{-T}(\boldsymbol{J}^T)^+\left(\begin{bmatrix} m_p\boldsymbol{E}_3 & \\ & {}^o\boldsymbol{I}_p \end{bmatrix} + \sum_{i=1}^{8}\boldsymbol{J}_{iv}^T m_i \boldsymbol{J}_{iv} + \sum_{i=1}^{8}\boldsymbol{J}_{i\omega}^T {}^i\boldsymbol{I}_i \boldsymbol{J}_{i\omega}\right)$$
$$+\boldsymbol{A}^{-T}\mathrm{diag}(m_{q1} \quad m_{q2} \quad m_{q3} \quad m_{q4} \quad m_{q5} \quad m_{q6} \quad m_{q7} \quad m_{q8})\boldsymbol{J} + \boldsymbol{A}\boldsymbol{I}_{LCM}\boldsymbol{J}$$
$$= [\boldsymbol{M}_1 \quad \boldsymbol{M}_2 \quad \boldsymbol{M}_3 \quad \boldsymbol{M}_4 \quad \boldsymbol{M}_5 \quad \boldsymbol{M}_6] \tag{60}$$

is the generalized inertia matrix of the redundant parallel manipulator, which maps the acceleration of the moving platform into the actuating torques. $\boldsymbol{E}_3$ denotes the unit matrix of order three. $\boldsymbol{V}(\boldsymbol{X}, \dot{\boldsymbol{X}})$ and $\boldsymbol{g}(\boldsymbol{X})$ are the velocity term and the gravity term of the inverse dynamic equations, respectively.

When the acceleration and the velocity of the moving platform are the unit vector along $\boldsymbol{\chi}$, the actuating torques caused by the respective acceleration, velocity, and gravity term are

$$\boldsymbol{\tau}_{a\chi_j} = \boldsymbol{M}(\boldsymbol{X})\boldsymbol{\chi}_j = \boldsymbol{M}_j, \quad j = 1, 2, \ldots, 6. \tag{61}$$

$$\boldsymbol{\tau}_{v\chi_j} = \boldsymbol{V}(\boldsymbol{X}, \dot{\boldsymbol{X}})\Big|_{\dot{\boldsymbol{X}}=\boldsymbol{\chi}_j, \quad j=1,2,\ldots,6}, \tag{62}$$

$$\boldsymbol{\tau}_g = \boldsymbol{g}(\boldsymbol{X}). \tag{63}$$

For the ith input joint

$$\tau_{ia\chi_j} = \Big[\underbrace{0\cdots0}_{i-1} \quad 1 \quad \underbrace{0\cdots0}_{8-i}\Big]\boldsymbol{M}_j = \boldsymbol{M}_{ij}, \tag{64}$$

$$\tau_{iv\chi_j} = \Big[\underbrace{0\cdots0}_{i-1} \quad 1 \quad \underbrace{0\cdots0}_{8-i}\Big]\boldsymbol{\tau}_{v\chi_j}, \tag{65}$$

$$\tau_{ig} = \Big[\underbrace{0\cdots0}_{i-1} \quad 1 \quad \underbrace{0\cdots0}_{8-i}\Big]\boldsymbol{\tau}_g, \tag{66}$$

so,

$$\tau_{ia\,\max} = \max([|\boldsymbol{M}_{i1}|, \quad |\boldsymbol{M}_{i2}|, \ \ldots, |\boldsymbol{M}_{i6}|])$$
$$= \max\left(\left[\left|\tau_{ia\chi_1}\right|, \quad \left|\tau_{ia\chi_2}\right|, \ \ldots, \left|\tau_{ia\chi_6}\right|\right]\right), \tag{67}$$

$$\tau_{iv\,\max} = \max\left(\left[\left|\tau_{iv\chi_1}\right|, \quad \left|\tau_{iva\chi_2}\right|, \ \ldots, \left|\tau_{iva\chi_6}\right|\right]\right), \tag{68}$$

$$\tau_{ig\,\max} = \left|\tau_{ig}\right| \tag{69}$$

are the maximum actuating torques of the ith joint caused by the respective acceleration, velocity, and gravity term.

Thus

$$\tau_{i\,\max} = \tau_{ia\,\max} + \tau_{iv\,\max} + \tau_{ig\,\max} \tag{70}$$

is the maximum actuating torque of the ith joint when the acceleration and the velocity of the moving platform are unit. It is taken as the performance index to evaluate the ith joint torque capability of the redundant parallel manipulator.

4.2.2. Joint power capability. When the acceleration and the velocity of the moving platform are the unit vector along $\boldsymbol{\chi}_1, \boldsymbol{\chi}_2, \ldots, \boldsymbol{\chi}_6$, the power of the ith input joint is

$$P_{i\chi_j} = \dot{\theta}_{i\chi_j}\tau_{ia\chi_k v\chi_j g}, \tag{71}$$

where

$$\tau_{ia\chi_k v\chi_j g} = \tau_{ia\chi_k} + \tau_{iv\chi_j} + \tau_{ig}, \quad 1 \le k, \quad j \le 6, \tag{72}$$

so

$$P_{i\,\max}$$
$$= \max\left(\left[\left|\dot{\theta}_{i\chi_1}\tau_{iav\chi_1 g}\right|, \quad \left|\dot{\theta}_{i\chi_2}\tau_{iav\chi_2 g}\right|, \ \ldots, \left|\dot{\theta}_{i\chi_6}\tau_{iav\chi_6 g}\right|\right]\right), \tag{73}$$

where

$$\tau_{iav\chi_j g} = \tau_{ia\,\max} + \left|\tau_{iv\chi_j}\right| + \tau_{ig\,\max}. \tag{74}$$

$P_{i\,\max}$ is the maximum power of the ith joint when the acceleration and the velocity of the moving platform are unit. It is taken as the performance index to evaluate the ith joint power capability of the redundant parallel manipulator.

4.3. General case

When the maximum translational motion of the moving platform along x, y, and z axes and the maximum rotational motion about x, y, and z axes are given as $\eta_{k\,k=1,2,\ldots,6}$ m/s^2(rad/s^2) and $\lambda_{j\,j=1,2,\ldots,6}$ m/s(rad/s) in the task space, these indices to evaluate the ith input joint capability are

$$\dot{\theta}_{i\,\max} = \max\left(\left[\left|\lambda_1\dot{\theta}_{i\chi_1}\right|, \quad \left|\lambda_2\dot{\theta}_{i\chi_2}\right|, \ldots, \left|\lambda_6\dot{\theta}_{i\chi_6}\right|\right]\right), \tag{75}$$

$$\tau_{i\,\max} = \max\left(\left|\eta_k\tau_{ia\chi_k}\right| + \lambda_j^2\left|\tau_{iv\chi_j}\right| + \tau_{ig\,\max}\right), \tag{76}$$

$$P_{i\,\max}$$
$$= \max\left(\left[\left|\lambda_1\dot{\theta}_{i\chi_1}\tau_{iav\chi_1 g}\right|, \left|\lambda_2\dot{\theta}_{i\chi_2}\tau_{iav\chi_2 g}\right|, \ldots, \left|\lambda_6\dot{\theta}_{i\chi_6}\tau_{iav\chi_6 g}\right|\right]\right), \tag{77}$$

where

$$\tau_{iav\chi_j g} = \eta_k\tau_{ia\,\max} + \lambda_j^2\left|\tau_{iv\chi_j}\right| + \tau_{ig\,\max}. \tag{78}$$

The redundant parallel manipulator has better performance when these indices above are smaller.

In order to evaluate the ith input joint capability of the redundant parallel manipulator in different directions with different instantaneous velocity and acceleration, these indices are adopted as

$$\dot{\theta}_{i\lambda_j\chi_j} = \left|\lambda_j\dot{\theta}_{i\chi_j}\right|, \tag{79}$$

$$\tau_{ia\eta_k\chi_k v\lambda_j\chi_j g} = \left|\eta_k\tau_{ia\chi_k}\right| + \lambda_j^2\left|\tau_{iv\chi_j}\right| + \left|\tau_{ig}\right|, \tag{80}$$

$$P_{ia\eta_k\chi_k v\lambda_j\chi_j g} = \left|\lambda_j\dot{\theta}_{i\chi_j}\tau_{ia\eta_k\chi_k v\lambda_j\chi_j g}\right|. \tag{81}$$

https://doi.org/10.1017/S0263574710000330 Published online by Cambridge University Press

Table I. The parameters of the base platform (m).

	1	2	3	4	5	6	7	8
x_{Bi}	0.400000	0.400000	−0.400000	−0.400000	0.400000	−0.400000	−2.000000	−2.000000
y_{Bi}	−0.400000	0.400000	0.400000	−0.400000	−2.000000	−2.000000	−0.400000	0.400000
z_{Bi}	0.000000	0.000000	0.000000	0.000000	1.500000	1.500000	1.500000	1.500000

Table II. The parameters of the moving platform, which are measured in the coordinate frame $O' - u'v'w'$ (m).

	1	2	3	4	5	6	7	8
x_{Ai}	0.400000	0.400000	−0.400000	−0.400000	0.400000	−0.400000	−0.681000	−0.681000
y_{Ai}	−0.400000	0.400000	0.400000	−0.400000	−0.681000	−0.681000	−0.400000	0.400000
z_{Ai}	−0.166000	−0.166000	−0.166000	−0.166000	−0.037500	−0.037500	−0.037500	−0.037500

Table III. The length of the strut $C_i A_i$ (m).

	1	2	3	4	5	6	7	8
l_i	1.000000	1.000000	1.000000	1.000000	1.000000	1.000000	1.000000	1.000000

It is the input velocity, torque, and power of the respective actuated joint required for producing (1) a maximum linear and angular acceleration η_k m/s^2(rad/s^2); and (2) a maximum linear and angular velocity λ_j m/s(rad/s) of the moving platform. In order to control the respective joint capability of the redundant parallel manipulator in different directions, these indices can also be used for the constraint function in the dynamic optimum design.

If the maximum translational motion and the maximum rotational motion of the moving platform are assigned as $v_{\max}$, $\omega_{\max}$, $\dot{v}_{\max}$, and $\dot{\omega}_{\max}$, the ith input joint capability indices are

$$\begin{aligned} \dot{\theta}_{i\max} &= \max\left(\lambda \left|\dot{\theta}_{i\chi_j}\right|\right), \quad j = 1, 2, \ldots, 6, \\ & j = 1, 2, 3, \quad \lambda = v_{\max}, \\ & j = 4, 5, 6, \quad \lambda = \omega_{\max}, \end{aligned} \tag{82}$$

$$\begin{aligned} \tau_{i\max} &= \max\left(\left|\eta\tau_{ia\chi_k}\right| + \lambda^2 \left|\tau_{iv\chi_j}\right| + \tau_{ig\max}\right), \\ & j, k = 1, 2, \ldots, 6, \\ & j, k = 1, 2, 3, \quad \eta = \dot{v}_{\max}, \quad \lambda = v_{\max}, \\ & j, k = 4, 5, 6, \quad \eta = \dot{\omega}_{\max}, \quad \lambda = \omega_{\max}, \end{aligned} \tag{83}$$

$$\begin{aligned} P_{i\max} &= \max\left(\left|\lambda\dot{\theta}_{i\chi_j}\tau_{ia\eta\chi_k v\lambda\chi_j g}\right|\right), \quad j, k = 1, 2, \ldots, 6, \\ & j, k = 1, 2, 3, \quad \eta = \dot{v}_{\max}, \quad \lambda = v_{\max}, \\ & j, k = 4, 5, 6, \quad \eta = \dot{\omega}_{\max}, \quad \lambda = \omega_{\max}, \end{aligned} \tag{84}$$

where

$$\begin{aligned} \tau_{ia\eta\chi_k v\lambda\chi_j g} &= \eta\tau_{ia\max} + \lambda^2 \left|\tau_{iv\chi_j}\right| + \tau_{ig\max}, \\ & j, k = 1, 2, \ldots, 6, \\ & j, k = 1, 2, 3, \quad \eta = \dot{v}_{\max}, \quad \lambda = v_{\max}, \\ & j, k = 4, 5, 6, \quad \eta = \dot{\omega}_{\max}, \quad \lambda = \omega_{\max}. \end{aligned} \tag{85}$$

5. Simulation

In this section, the joint capability evaluation of the 8-PSS redundant parallel manipulator is investigated by simulation.

Table IV. The mass parameters of the manipulator (kg).

	1	2	3	4	5	6	7	8
m_i	20	20	20	20	20	20	20	20
m_{qi}	50	50	50	50	50	50	50	50

The parameters of the manipulator used for the simulation are given in Tables I–IV.

The mass of the moving platform is $m_p = 200$ kg. The inertia parameters used in the simulation are given as

$$^{o'}\boldsymbol{I}_p = \begin{bmatrix} 17.333 & 0 & 0 \\ 0 & 17.333 & 0 \\ 0 & 0 & 33.333 \end{bmatrix} \mathrm{kg} \cdot \mathrm{m}^2,$$

$$^{i}\boldsymbol{I}_i = \begin{bmatrix} 1.279 & 0 & 0 \\ 0 & 1.279 & 0 \\ 0 & 0 & 0.005 \end{bmatrix} \mathrm{kg} \cdot \mathrm{m}^2,$$

$I_{Li} = 10.5 \times 10^{-4}\,\mathrm{kg} \cdot \mathrm{m}^2$, $I_{Ci} + I_{Mi} = 248 \times 10^{-4}\,\mathrm{kg} \cdot \mathrm{m}^2$. Other parameters used in the simulation are given as $d_i = 0.244$ m and $z_0 = 1.744$ m.

The indices to evaluate the joint capability of the redundant parallel manipulator are computed when the pose of the moving platform are $\phi_x = \phi_y = \phi_z = 0$ and $z = z_0$. The desired maximum acceleration and velocity of the moving platform are

$$\begin{aligned} &\eta_1 = 6, \quad \eta_2 = 6, \quad \eta_3 = 9\,(\mathrm{m/s^2}) \\ &\eta_4 = 3, \quad \eta_5 = 3, \quad \eta_6 = 2\,(\mathrm{rad/s^2}) \end{aligned}$$

and

$$\begin{aligned} &\lambda_1 = 4, \quad \lambda_2 = 4, \quad \lambda_3 = 6\,(\mathrm{m/s}) \\ &\lambda_4 = 2, \quad \lambda_5 = 2, \quad \lambda_6 = 3\,(\mathrm{rad/s}). \end{aligned}$$

The indices of the joint velocity capability are shown in Table V.

Table V. The indices of the joint velocity capability in the investigated workspace (rad/s).

	1	2	3	4	5	6	7	8
$\dot{\theta}_{i\,\max}$	753.9822	753.9822	753.9822	753.9822	502.6548	502.6548	502.6548	502.6548

In this simulation, it is shown from Table V that (1) the velocity capability of the ith joint is constant in the investigated workspace when the pose of the moving platform are $\phi_x = \phi_y = \phi_z = 0$ and $z = z_0$. (2) The velocity capabilities of the joint $i(i = 1, 2, \ldots, 4)$ are equal to each other and the velocity capabilities of the joint $i(i = 5, 6, \ldots, 8)$ are also equal due to the symmetrical characteristics of the 8-PSS redundant parallel manipulator. (3) The joint $i(i = 5, 6, \ldots, 8)$ have better velocity capabilities than those of the joint $i(i = 1, 2, \ldots, 4)$.

The distributions of the joint dynamic capability are shown in Figs 4 and 5. It is shown that the joint $i(i = 1, 2, \ldots, 4)$ have better torque capabilities than those of the joint $i(i = 5, 6, \ldots, 8)$ while have worse power capabilities than those of the joint $i(i = 5, 6, \ldots, 8)$ in this simulation. It is shown that the eight input joints of the 8-PSS redundant parallel manipulator have different dynamic capabilities such as torque and power capabilities with respect to the configuration in the investigated workspace. Therefore, different kinds of motor can be equipped for the actuating joint of the prototype in order to reduce the cost.

6. Conclusions

This paper investigates the joint velocity, torque, and power capability of the 8-PSS redundant parallel manipulator by simulation. The conclusions are drawn as follows.

(1) A series of new indices with obvious physical meanings have been presented to evaluate the respective joint velocity, torque, and power capability of the redundant parallel manipulator. The torque index used to evaluate the respective joint dynamic capability of the redundant parallel manipulator is decoupled into the acceleration, velocity, and gravity term.

(2) The joint capability of the redundant parallel manipulator is evaluated by the velocity, torque, and power indices, so it is possible to control the respective joint capability of the redundant parallel manipulator by means of the dynamic optimum design.

(3) The results shown in the simulation demonstrate that the joint $i(i = 1, 2, \ldots, 4)$ have better velocity and torque capabilities than those of the joint $i(i = 5, 6, \ldots, 8)$ while have worse power capabilities than those of the joint $i(i = 5, 6, \ldots, 8)$. For the 8-PSS redundant parallel manipulators, the eight input joints have different dynamic capabilities such as torque and power capabilities with respect to the configuration in the investigated workspace.

Future investigation will study the dynamic optimum design of the redundant parallel manipulator by adopting the presented indices. However, these related issues will be addressed by separate papers.

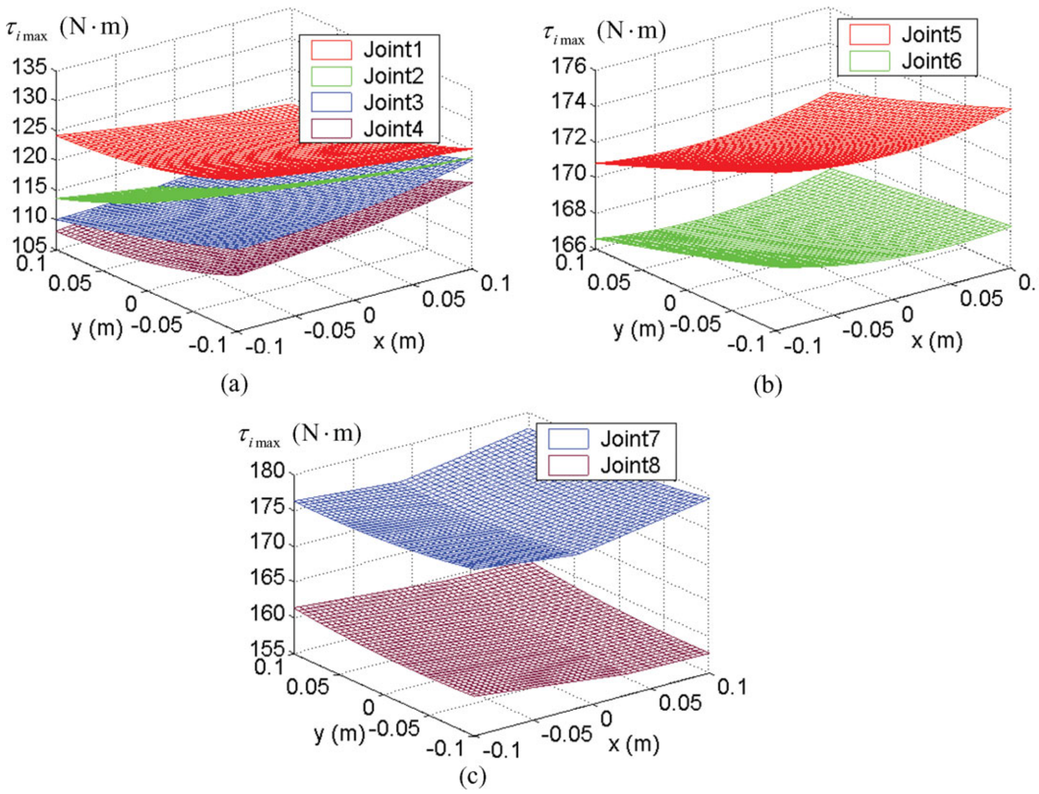

Figure 4. The distributions of the joint torque capability $\tau_{i\,\max}$.

https://doi.org/10.1017/S0263574710000330 Published online by Cambridge University Press

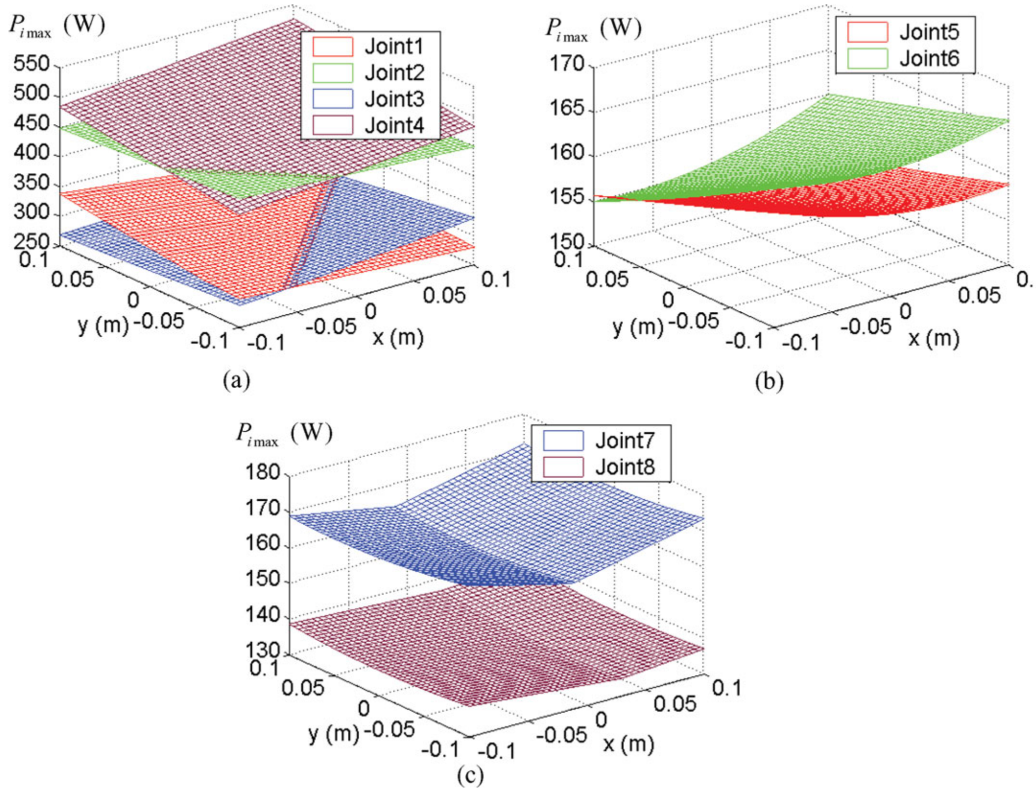

Figure 5. The distributions of the joint power capability $P_{i\,\max}$.

Acknowledgments
This research is jointly sponsored by the National Natural Science Foundation of China (Grant No. 50905102), the China Postdoctoral Science Foundation (Grant No. 200801199), and the Natural Science Foundation of Guangdong Province (Grant No. 8351503101000001). The authors would also like to thank the anonymous reviewers for their very useful comments.

References

1. J. P. Merlet, "Jacobian, Manipulability, condition number, and accuracy of parallel robots," *ASME J. Mech. Des.* **128**(1), 199–206 (2006).
2. J. P. Merlet, "Parallel robot: Open problems," [Online]. Available: http://www-sop.inria.fr/coprin/equipe/merlet/merlet_eng.html. (1999).
3. J. P. Merlet, "Still a long way to go on the road for parallel mechanisms," [Online]. Available: http://www-sop.inria.fr/coprin/equipe/merlet/merlet_eng.html. (2002).
4. C. M. Gosselin and J. Angeles, "The optimum kinematic design of a planar three-degree-of-freedom parallel manipulators," *ASME J. Mech. Transm. Autom. Des.* **110**(1), 35–41 (1988).
5. C. M. Gosselin and J. Angeles, "The optimum kinematic design of a spherical three Degree-of-Freedom parallel manipulator," *ASME J. Mech. Transm. Autom. Des.* **111**(2), 202–207 (1989).
6. C. M. Gosselin and J. Angeles, "A global performance index for the kinematic optimization of robotic manipulators," *ASME J. Mech. Des.* **113**(3), 220–226 (1991).
7. H. Lipkin and J. Duffy, "Hybrid twist and wrench control for a robotic manipulator," *ASME J. Mech. Transm. Autom. Des.* **110**(6), 138–144 (1988).
8. K. L. Doty, C. Melchiorri and C. Bonevento, "A theory of generalized inverse applied to robotics," *Int. J. Rob. Res.* **12**(1), 1–19 (1993).
9. K. L. Doty, C. Melchiorri and E. M. Schwartz, "Robot manipulability," *IEEE Trans. Robot. Autom.* **11**(3), 462–468 (1995).
10. C. M. Gosselin, "Dexterity Indices for Planar and Spatial Robotic Manipulators," *Proceedings of the 1990 IEEE International Conference on Robotics and Automation*, Cincinnati, USA (1990) pp. 650–655.
11. G. Pond and J. A. Carretero, "Formulating Jacobian matrices for the dexterity analysis of parallel manipulators," *Mech. Mach. Theory* **41**(9), 1505–1519 (2006).
12. O. Altuzarra, O. Salgado and V. Petuya, "Point-based Jacobian formulation for computational kinematics of manipulators," *Mech. Mach. Theory* **41**(12), 1407–1423 (2006).
13. S. G. Kim and J. Ryu, "New dimensionally homogeneous Jcaobian matrix formulation by three end-effector points for optimal design of parallel manipulators," *IEEE Trans. Robot. Autom.* **19**(4), 731–737 (2003).
14. T. Yoshikawa, "Manipulability of robotic mechanisms," *Int. J. Robot. Res.* **4**(2), 3–9 (1985).
15. T. Yoshikawa, "Translational and Rotational Manipulability of Robotic Manipulators," *Proceedings of the American Control Conference*, San Diego, USA (1991) pp. 1070–1075.
16. K. S. Hong and J. G. Kim, "Manipulability analysis of a parallel machine tool: application to optimal link length design," *J. Robot. Syst.* **17**(8), 403–415 (2000).
17. O. Ma and J. Angeles, "The Concept of Dynamics Isotropy and its Applications to Inverse Kinematics and Trajectory Planning," *Proceedings of the 1990 IEEE International Conference on Robotics and Automation*, Cincinnati, USA (1990) pp. 481–486.
18. O. Ma and J. Angeles, "Optimum Design of Manipulators Under Dynamic Isotropy Conditions," *Proceedings of the 1993 IEEE International Conference on Robotics and Automation*, Atlanta, USA (1993) pp. 470–475.
19. H. Asada, "A geometrical representation of manipulator dynamics and its application to arm design," *ASME J. Dyn. Syst. Meas. Control* **105**(3), 131–135 (1983).

20. H. Asada, "Dynamic Analysis and Design of Robot Manipulators Using Inertia Ellipsoids," *Proceedings of the 1984 IEEE International Conference on Robotics and Automation*, Atlanta, USA (1984) pp. 94–102.
21. T. Yoshikawa, "Dynamic manipulability of robot manipulators," *J. Robot. Syst.* **2**(1), 113–124 (1985).
22. M. Li, T. Huang and J. P. Mei, "Dynamic formulation and performance comparison of the 3-DOF modules of two reconfigurable PKMs—the TriVariant and the Tricept," *ASME J. Mech. Des.* **127**(6), 1129–1136 (2005).
23. T. Huang, J. P. Mei and Z. X. Li, "A method for estimating servomotor parameters of a parallel robot for rapid pick-and-place operations," *ASME J. Mech. Des.* **127**(7), 596–601 (2005).
24. P. Chiacchio and M. Concilio, "The Dynamics Manipulability Ellipsoid for Redundant Manipulators," *Proceedings of the 1998 IEEE International Conference on Robotics and Automation*, Leuven, Belgium (1998) pp. 95–100.
25. P. Chiacchio, S. Chiaverini and L. Sciavicco, "Reformulation of Dynamic Manipulability Ellipsoid for Robotic Manipulators," *Proceedings of the 1991 IEEE International Conference on Robotics and Automation*, California, USA (1991) pp. 2192–2197.
26. F. C. Park and J. W. Kim, "Manipulability of closed kinematic chains," *ASME J. Mech. Des.* **120**(4), 542–548 (1998).
27. R. D. Gregorio and V. Parenti-Castelli, "Dynamic Performance Characterization of Three-Dof Parallel Manipulators," **In:** *Advances in Robot Kinematics: Theory and Applications* (J. Lenarcic and F. Thomas, eds.) (Kluwer Academic Publishers, Netherlands, 2002) pp. 11–20.
28. J. Kim, F. C. Park and S. J. Ryu, "Design and analysis of a redundantly actuated parallel mechanism for rapid machining," *IEEE Trans. Robot. Autom.* **17**(4), 423–434 (2001).
29. J. P. Merlet, "Redundant parallel manipulators," *Lab. Robot. Autom.* **8**(1), 17–24 (1996).
30. S. B. Nokleby, R. Fisher and R. P. Podhorodeski, "Force capabilities of redundantly-actuated parallel manipulators," *Mech. Mach. Theory* **40**(5), 578–599 (2005).
31. J. Wang and C. M. Gosselin, "Kinematic analysis and design of kinematically redundant parallel mechanisms," *ASME J. Mech. Des.* **126**(1), 109–118 (2004).
32. H. Cheng, Y. K. Yiu and Z. X. Li, "Dynamics and control of redundantly actuated parallel manipulators," *IEEE Trans. Mech.* **8**(4), 483–491 (2003).
33. Z. Huang and X. W. Kong, "Kinematic analysis on the spatial parallel mechanisms with redundant degree of freedom," *Chin. J. Mech. Eng.* **31**(3), 44–50 (1995).
34. A. Müller, "Internal preload control of redundantly actuated parallel manipulators—its application to backlash avoiding control," *IEEE Trans. Robot.* **21**(4), 668–677 (2005).
35. M. G. Mohamed and C. M. Gosselin, "Design and analysis of kinematically redundant parallel manipulators with configurable platforms," *IEEE Trans. Robot.* **21**(3), 277–287 (2005).
36. I. Ebrahimi, J. A. Carretero and R. Boudreau, "3-PRRR redundant planar parallel manipulator: Inverse displacement, workspace and singularity analyses," *Mech. Mach. Theory* **42**(8), 1007–1016 (2007).
37. K. E. Zanganeh and J. Angeles, "Mobility and Position Analyses of a Novel Redundant Parallel Manipulator," *Proceeding of the 1994 IEEE International Conference on Robotics and Automation*, California, USA (1994) pp. 3049–3054.
38. L. W. Tsai, "Solving the inverse dynamics of a Stewart-Gough manipulator by the principle of virtual work," *ASME J. Mech. Des.* **122**(1), 3–9 (2000).